PROBING THE NEUTRON SKIN WITH ULTRARELATIVISTIC ISOBARIC COLLISIONS

HAOJIE XU (徐浩洁)

HUZHOU UNIVERSITY(湖州师范学院)

IN COLLABORATION WITH:

LIE-WEN CHEN, HANLIN LI, ZIWEI LIN, CAIWAN SHEN, FUQIANG WANG, XIAOBAO WANG, HANZHONG ZHANG, JIE ZHAO, YING ZHOU.

THE 127TH HENPIC SEMINAR, NOV. 12, 2020

Outlines

- Introduction
- Isobar density and CME observables
- Neutron skin and multiplicity distributions
- Summary

arXiv: 1710.03086, arXiv:1808.06711, arXiv:1910.06170

I. Introduction

Heavy ion collisions

- Nuclear densities
- Collision evolution
  - Thermalization + Hydrodynamic
  - Transport
- Produced particles
  - Flow
  - High order cumulants
  - …

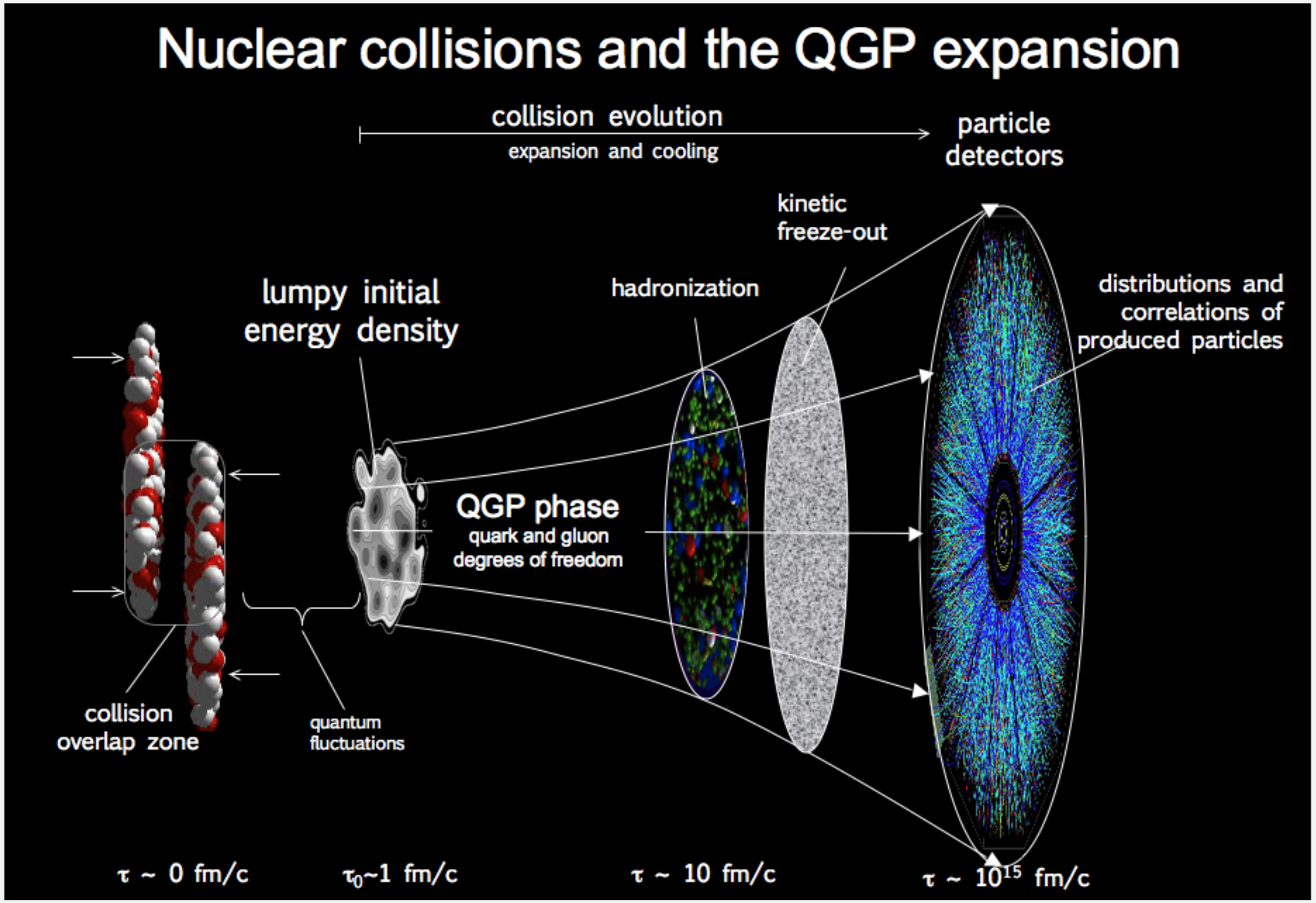

Nuclear densities

- Woods-Saxon distributions

$$\rho(r) = \rho_0 \frac{1 + w\left(\frac{r}{R}\right)^2}{1 + e^{(r-R)/a}}$$

Nucleus	R [fm]	a [fm]	w [fm]
^{2}H	0.01	0.5882	0
^{16}O	2.608	0.513	-0.51
^{28}Si	3.34	0.580	-0.233
^{32}S	2.54	2.191	0.16
^{40}Ca	3.766	0.586	-0.161
^{58}Ni	4.309	0.517	-0.1308
^{62}Cu	4.2	0.596	0
^{186}W	6.58	0.480	0
^{197}Au	6.38	0.535	0
^{207}Pb[a]	6.62	0.546	0
^{238}U	6.81	0.6	0

WS parameters used for the Monte Carlo Glauber model

arXiv:0805.4411

Nuclear charge density distributions can be obtained by the electron scatting experiment

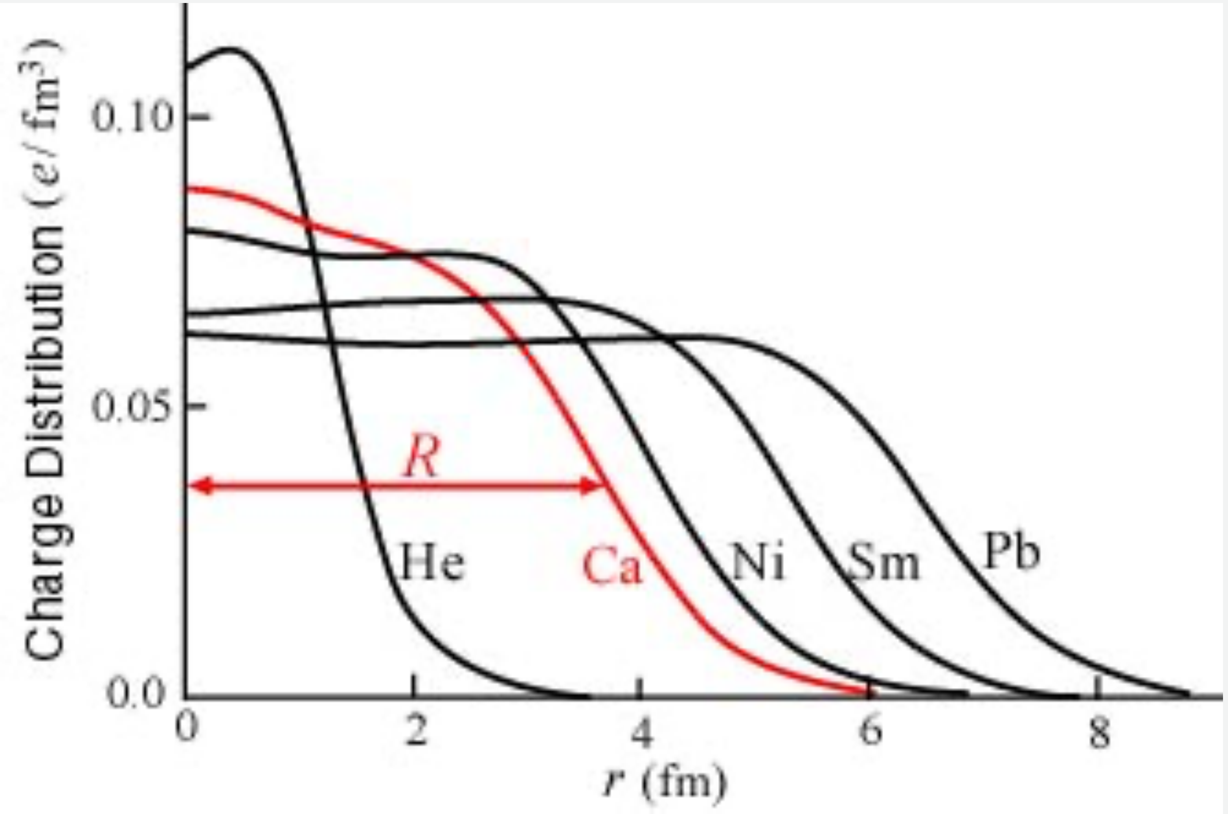

Collision geometry and anisotropic flow

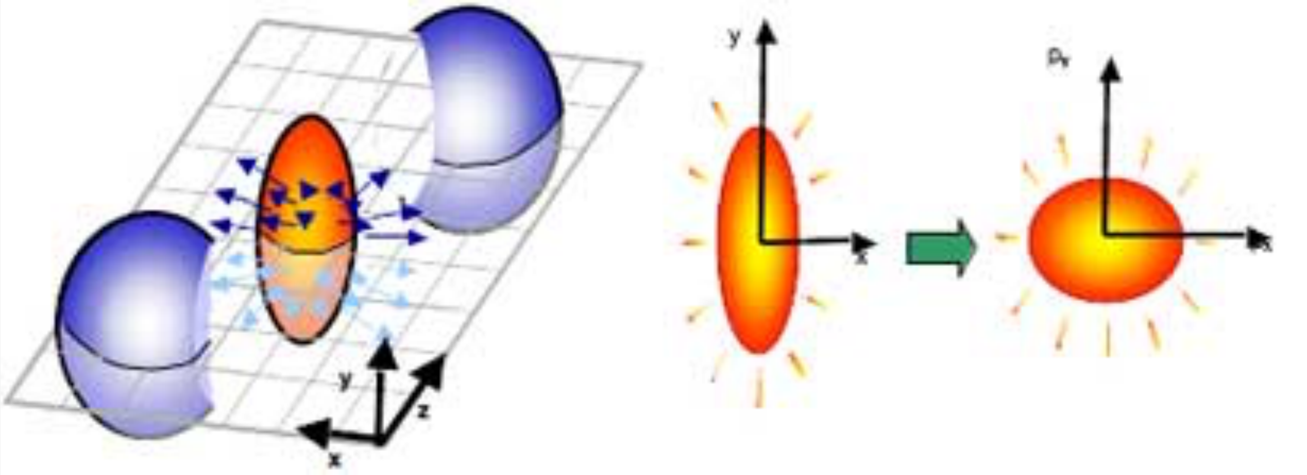

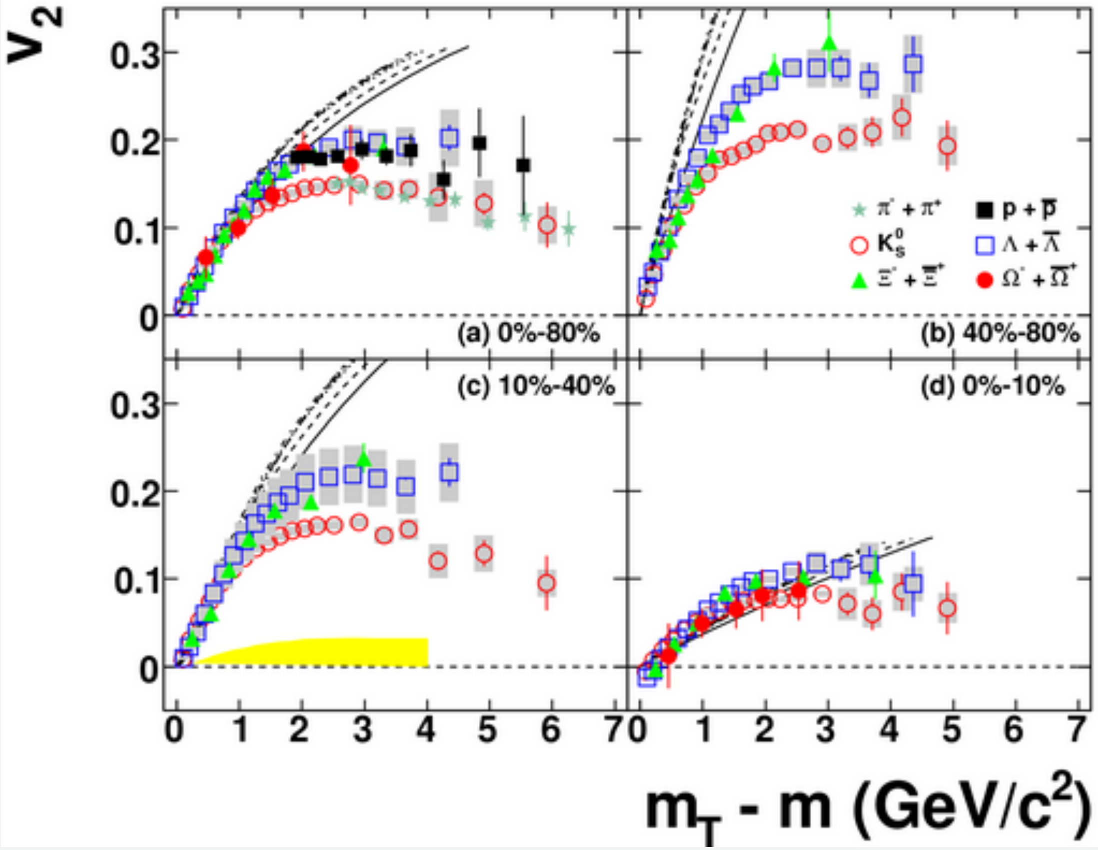

With the WS densities, we have made very successful connections between the final flow observable and the initial collision geometry.

$$\frac{dN}{d\phi} = N(1 + 2\sum_n v_n \cos[n(\phi - \Psi_n)]))$$

Prefect fluid - strong coupling QGP (sQGP)

STAR, PRC 77, 054901 (2018)

Effect of deformation

$$\rho(r) = \frac{\rho_0}{1 + \exp[\frac{r - R(1 + \beta_2 Y_{20} + \beta_4 Y_{40})}{a}]}$$

Au: $\beta_2 = -0.131$; U: $\beta_2 = 0.28$

Knee structure of v2 distributions at most-central U+U collisions

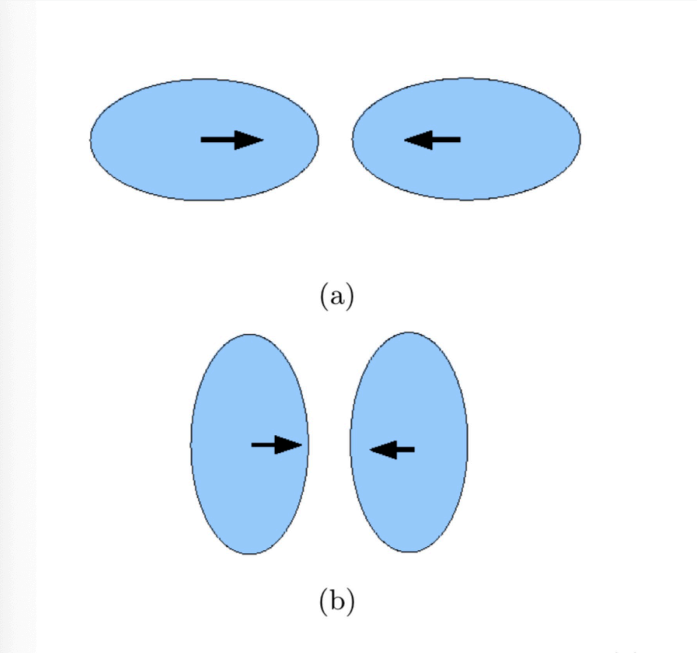

Small v_2 →

Large v_2 →

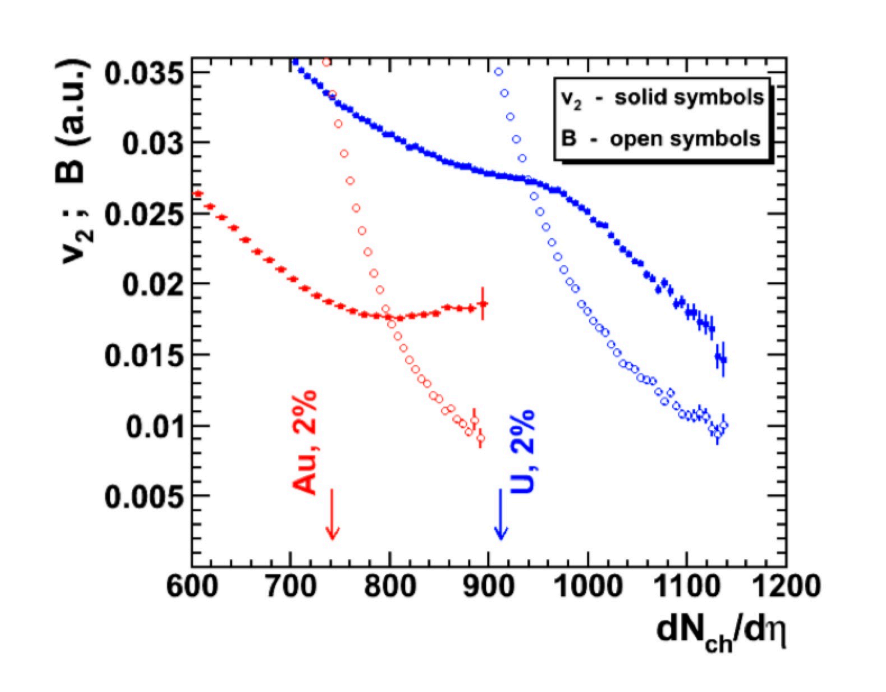

S. Voloshin, PRL105, 172301 (2010)

Probe the nuclear deformation in HIC

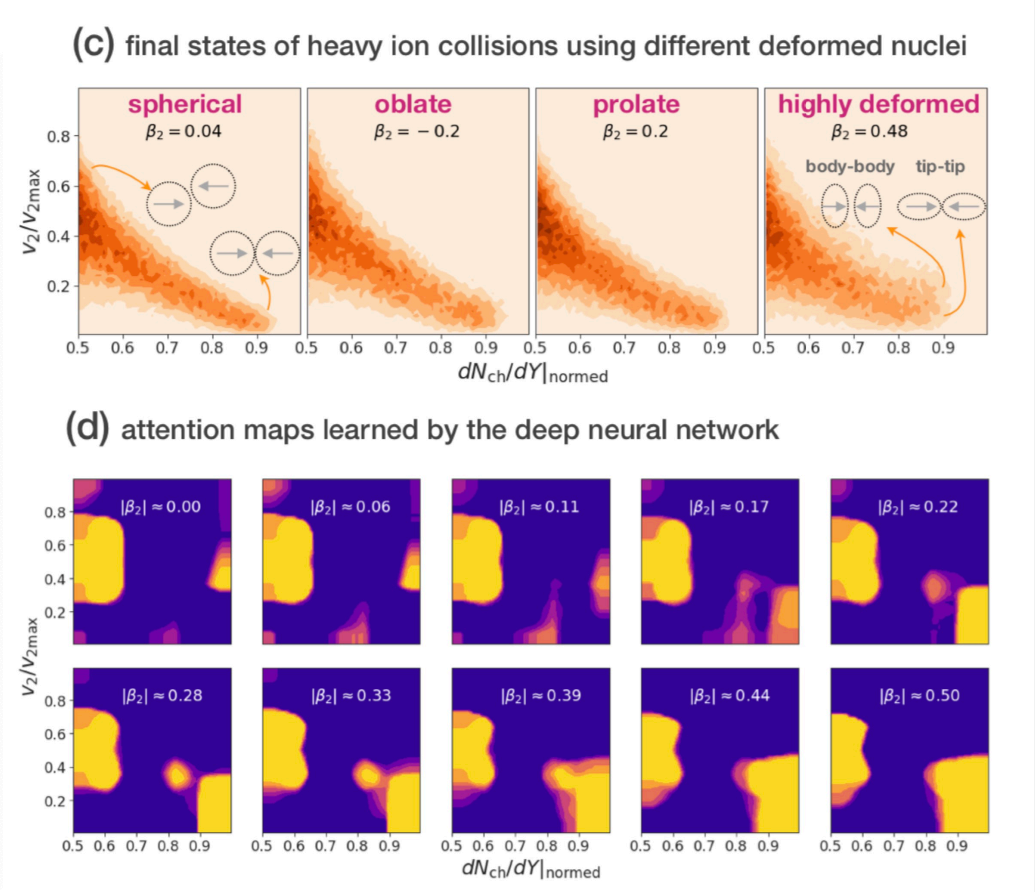

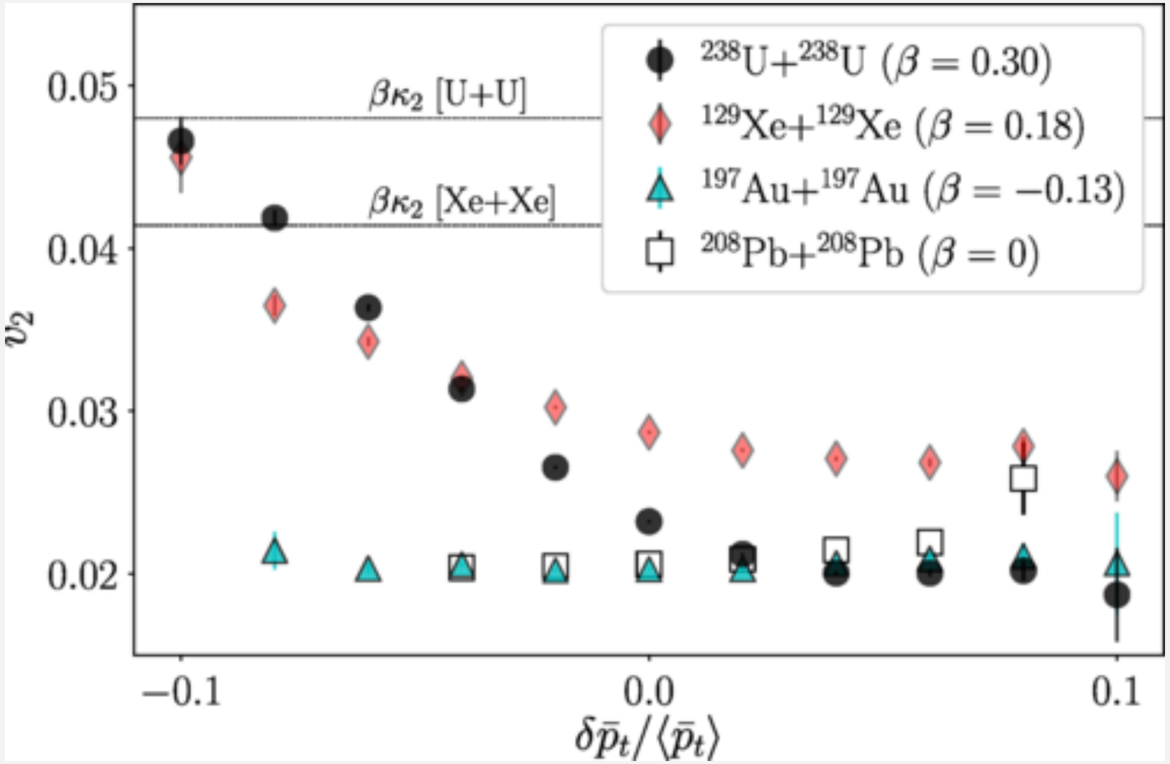

L. Pang, et.al , arXiv:1906.06429
(ds/dy, v2) deep neural network

G. Giacalone, PRL124, 202301 (2020)
Flow vs mean pt at most-central collisions

Effect of cluster correlations

$^{12}_{6}C + ^{208}_{82}Pb$

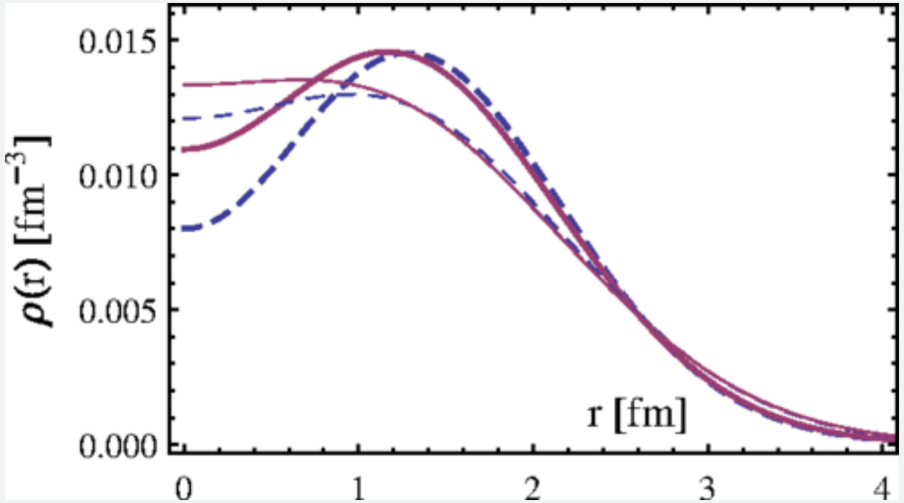

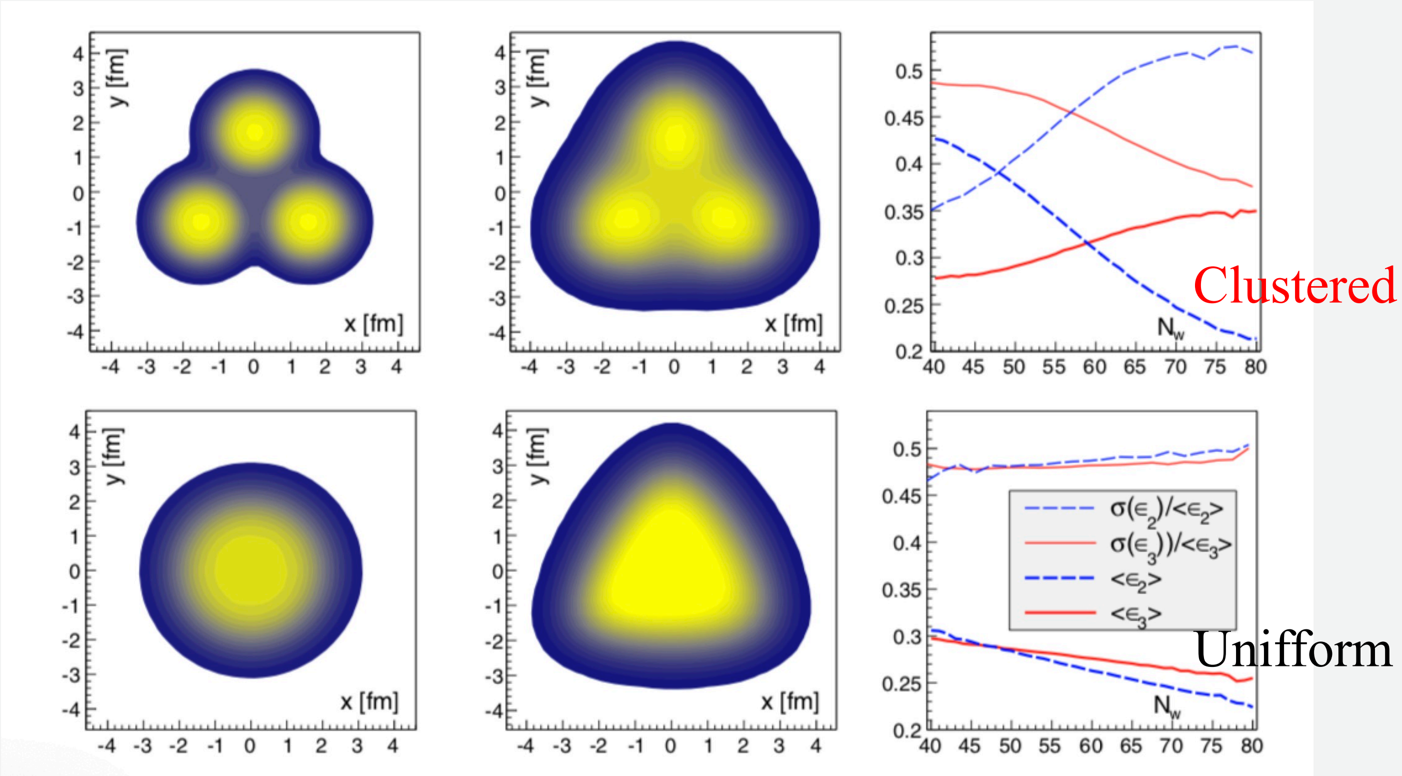

W. Broniowski, E. Arriola, PRL112, 112501 (2014)

The α-clustered and uniform 12C have very different predictions on v3, its event-by-event fluctuations, or the correlations of the v2 and v3

Isobar collisions

Woods-Saxon densities

The details of of the isobar densities could play a crucial role to investigate the tiny differences between isobar collisions .

DFT densities

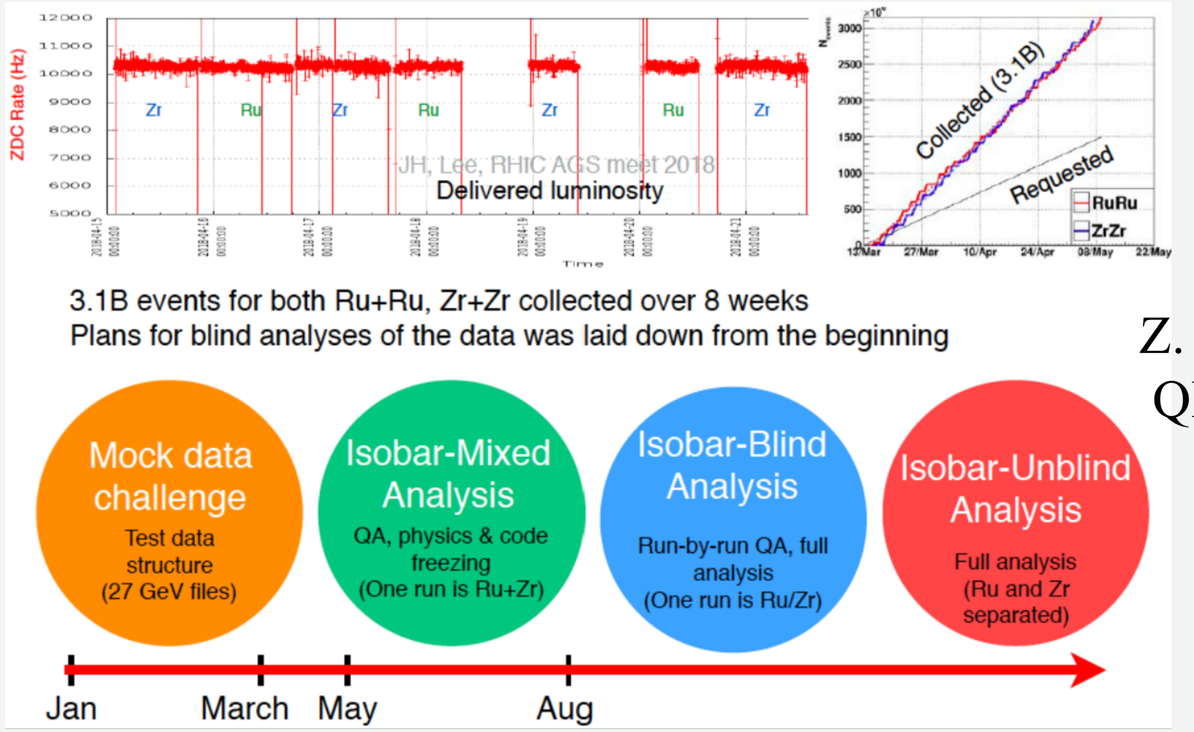

Z. Xu (STAR), QM2019

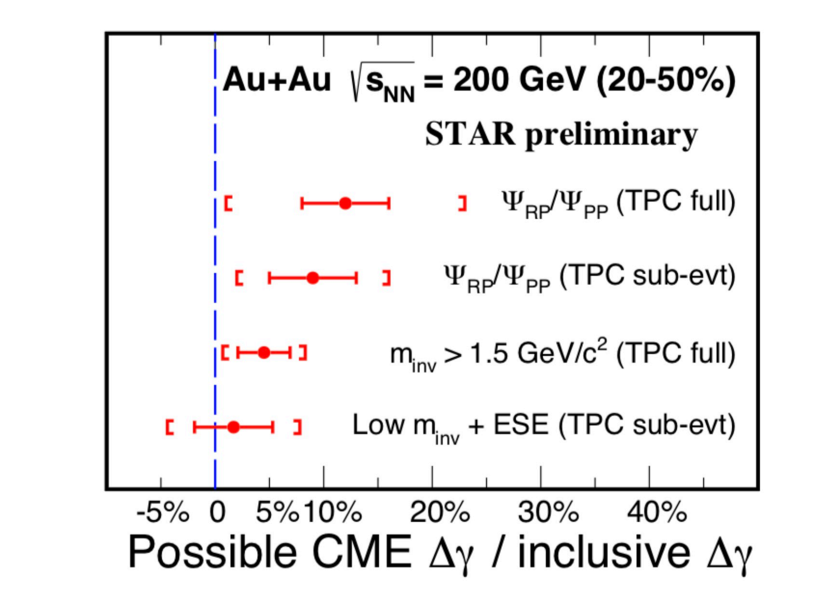

Zhao (STAR), NPA982, 535(2019)

II. Effect of isobar nuclear density on CME measurements

H. Xu, X. Wang, H. Li, J. Zhao, Z. Lin, C. Shen, F. Wang ,

“Importance of Isobar Density Distributions on the Chiral Magnetic Effect Search ”

Physical Review Letters, 121, 022301 (2018)

arXiv:1710.03086

Chiral magnetic effect

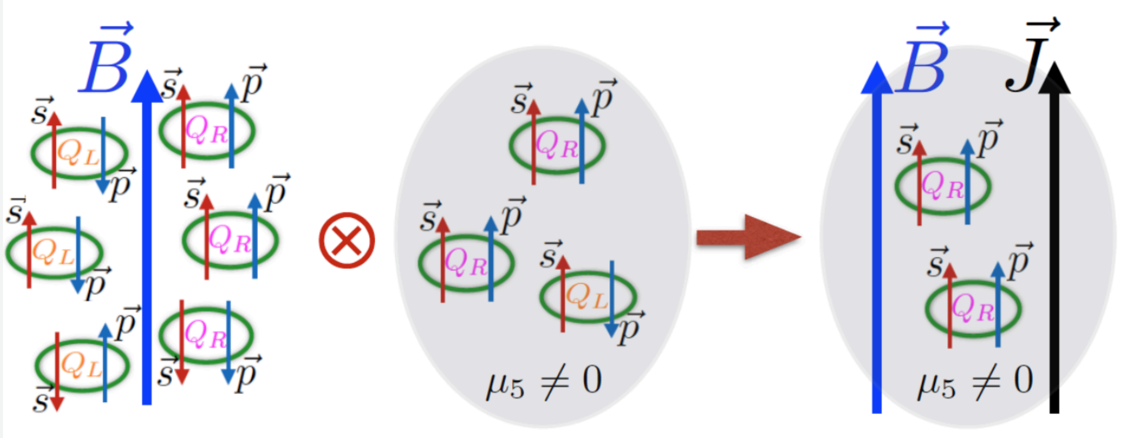

Chiral magnetic effect (CME)

$$\mathbf{J}_{\mathbf{cme}} = \sigma_5 \mathbf{B} = \left(\frac{(Qe)^2}{2\pi^2} \mu_5 \right) \mathbf{B},$$

D. Kharzeev, PPNP88, 1(2016)

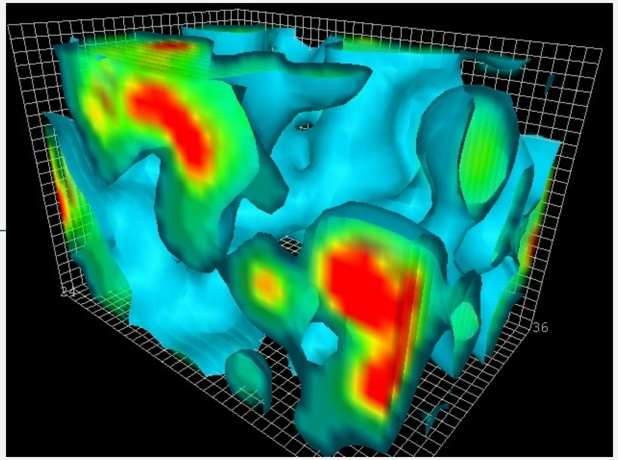

QCD Vacuum: Fluctuations of topological charge

$$Q_{\rm w} = \frac{g^2}{32\pi^2} \int d^4x\, F^a_{\mu\nu} \tilde{F}^{\mu\nu}_a$$

Strong magnetic field

$eB \sim m_\pi^2 @HIC$

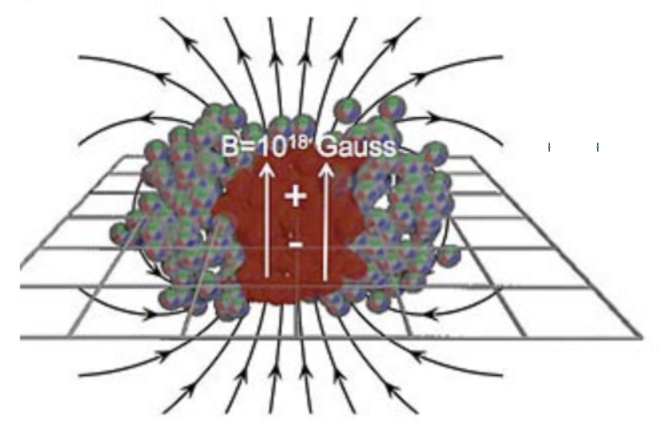

Signal and v_2 background

$$\gamma \equiv \langle \cos\left(\varphi_\alpha + \varphi_\beta - 2\Psi_{RP}\right)\rangle$$

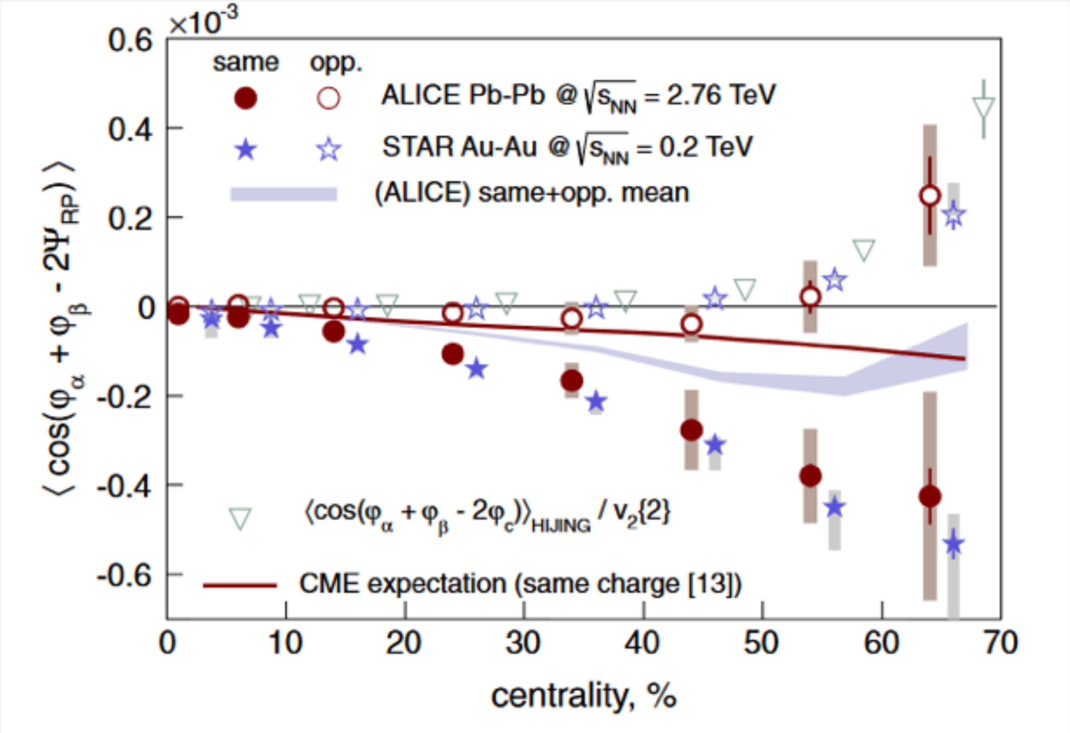

STAR, PRL103, 251601 (2009)
ALICE, PRL110, 012301 (2013)

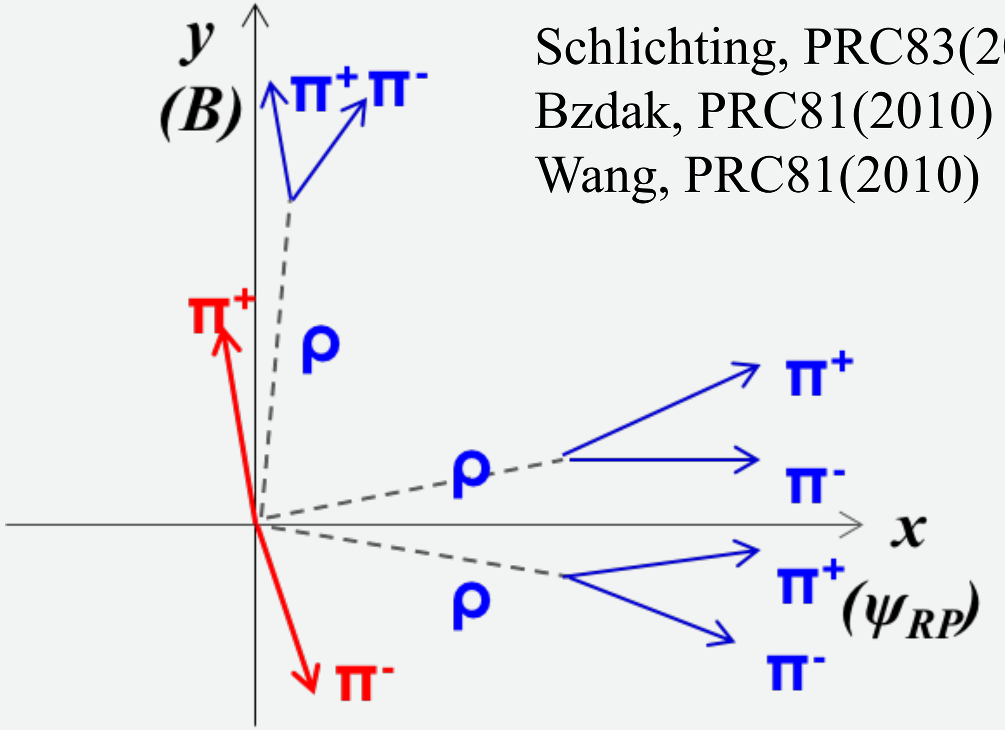

Schlichting, PRC83(2011)
Bzdak, PRC81(2010)
Wang, PRC81(2010)

Cluster decay + elliptic flow(v_2)

$$\begin{aligned} & \langle \cos(\phi_\alpha + \phi_\beta - 2\Psi_{RP})\rangle \\ \propto\ & \langle \cos(\phi_\alpha + \phi_\beta - 2\phi_\rho + 2\phi_\rho - 2\Psi_{RP})\rangle \\ \simeq\ & \langle \cos(\phi_\alpha + \phi_\beta - 2\phi_\rho)\rangle\langle 2(\phi_\rho - \Psi_{RP})\rangle \\ =\ & \langle \cos(\phi_\alpha + \phi_\beta - 2\phi_\rho)\rangle v_2^\rho \end{aligned}$$

Isobar collisions

The isobar collisions was proposed to measure the chiral magnetic effect.
S. Voloshin, PRL105, 172301 (2010)

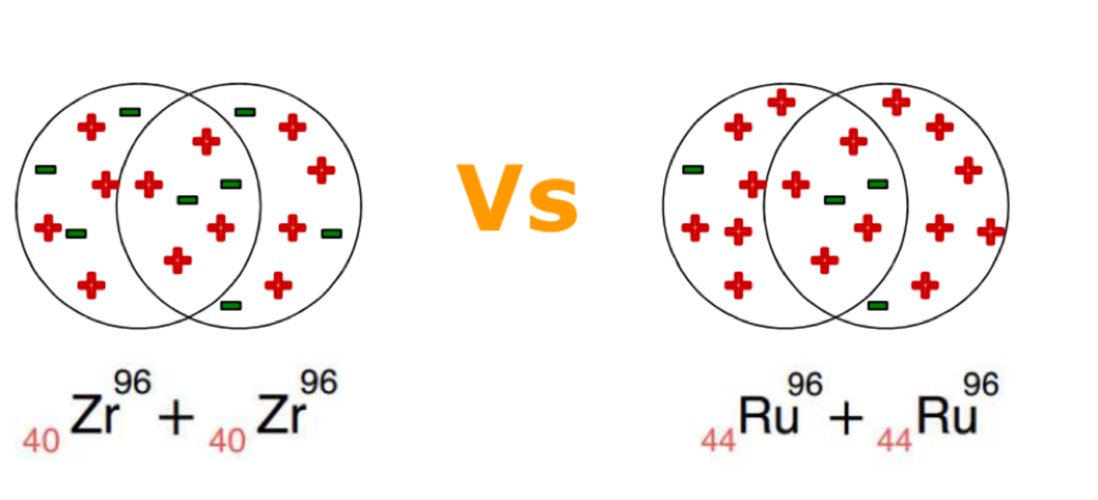

W. Deng, X. Huang, PRC94, 041901(2016)

	R	a	β_2
Zr	5.02	0.46	0.08/0.217
Ru	5.085	0.46	0.158/0.053

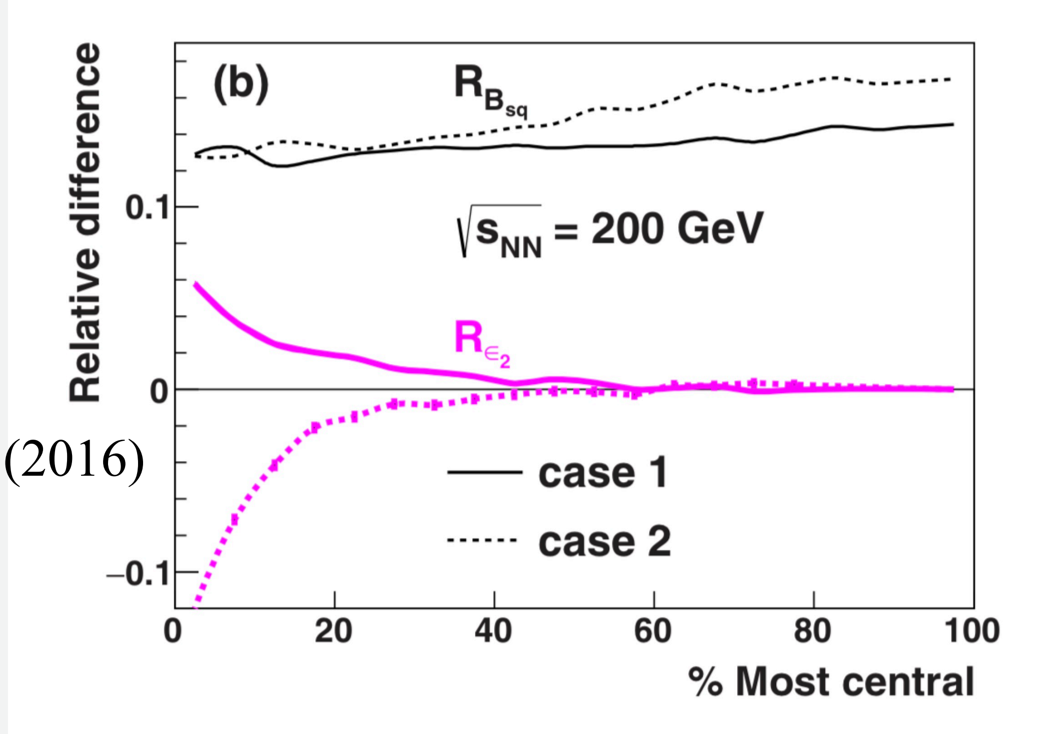

- Same eccentricities => flow background
- Different magnetic field => CME signals

CME measured in Au+Au collisions

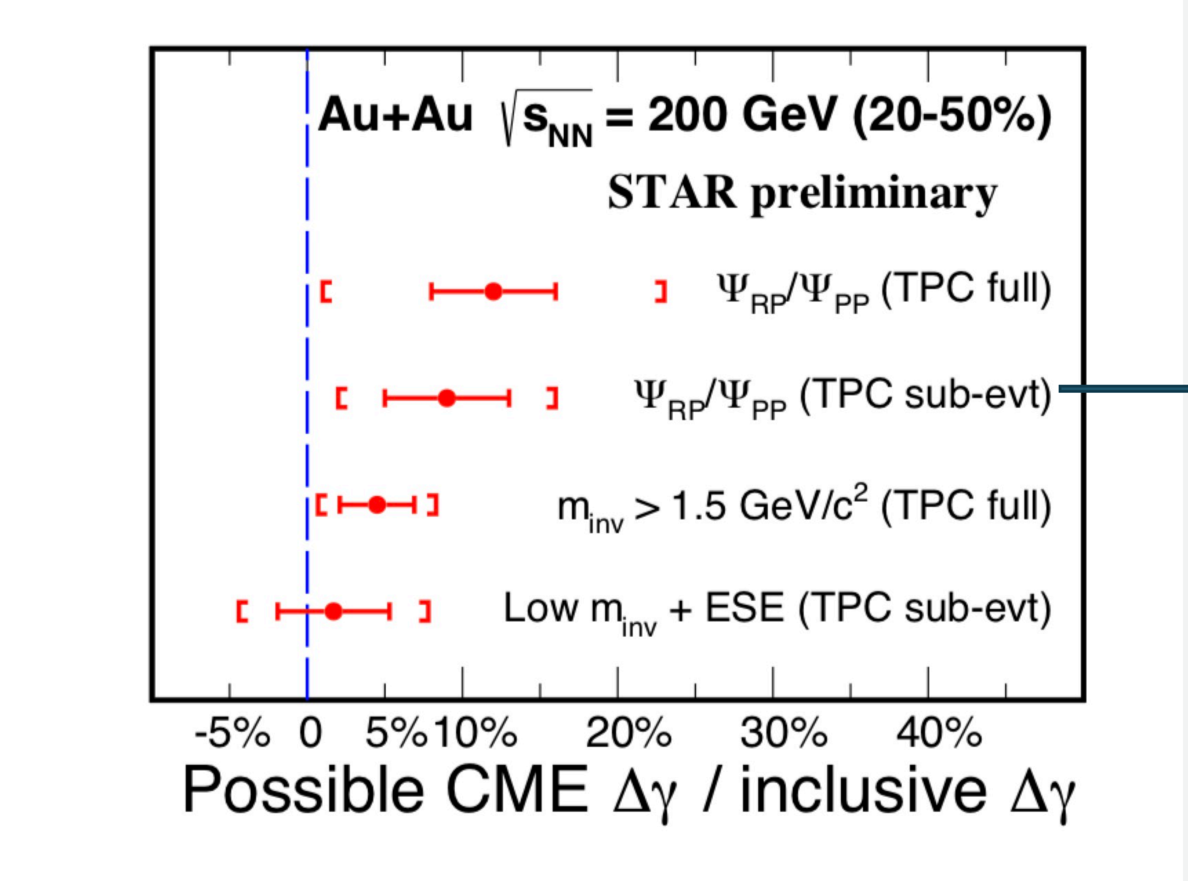

J. Zhao (STAR), NPA982, 535(2019)

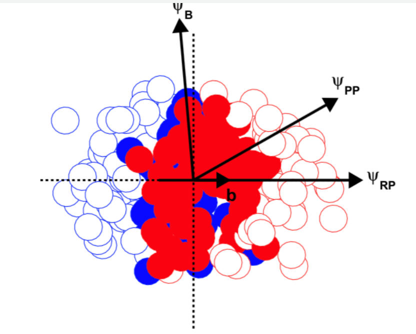

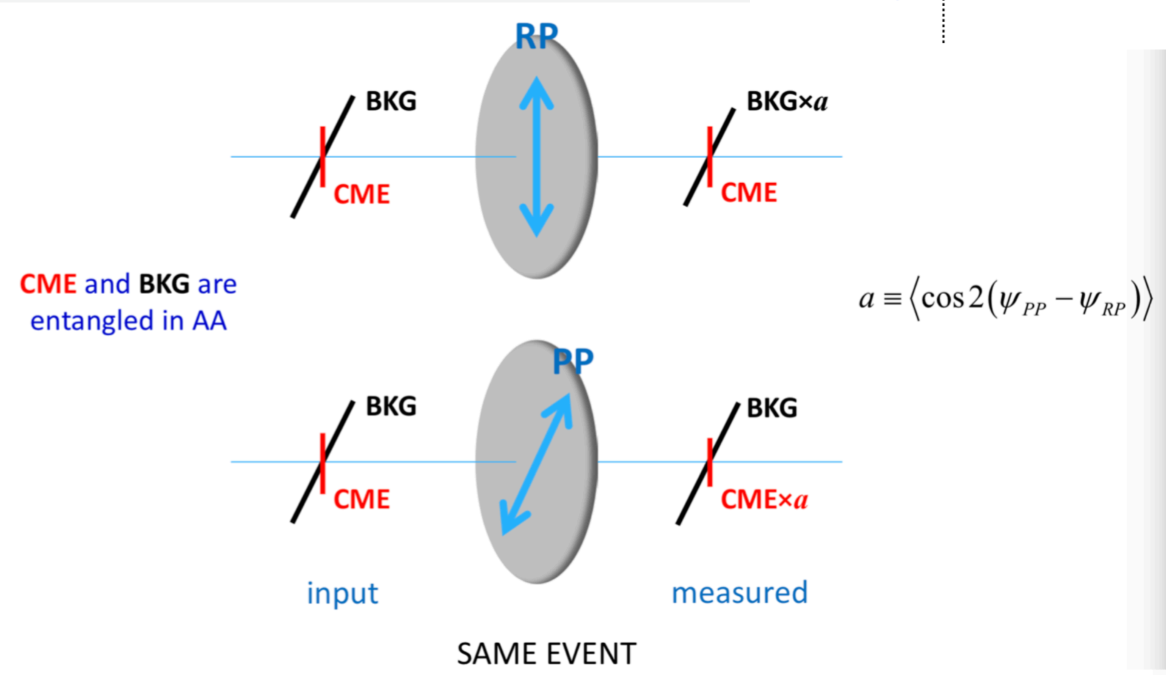

H. Xu, et.al, CPC42, 084103 (2018)

Background dominated

--- The CME signal, if exist, is very small

DFT densities VS WS densities

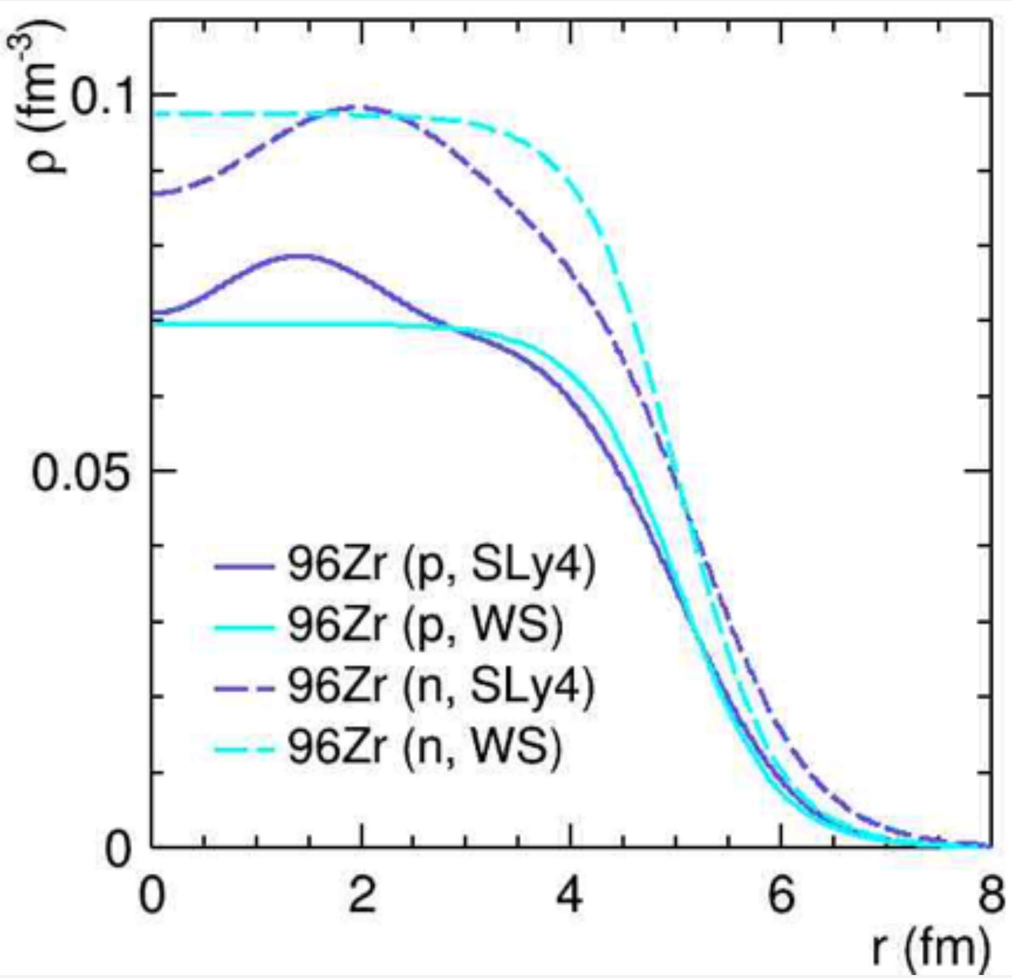

H. Xu, et.al, PRL121, 022301 (2018)

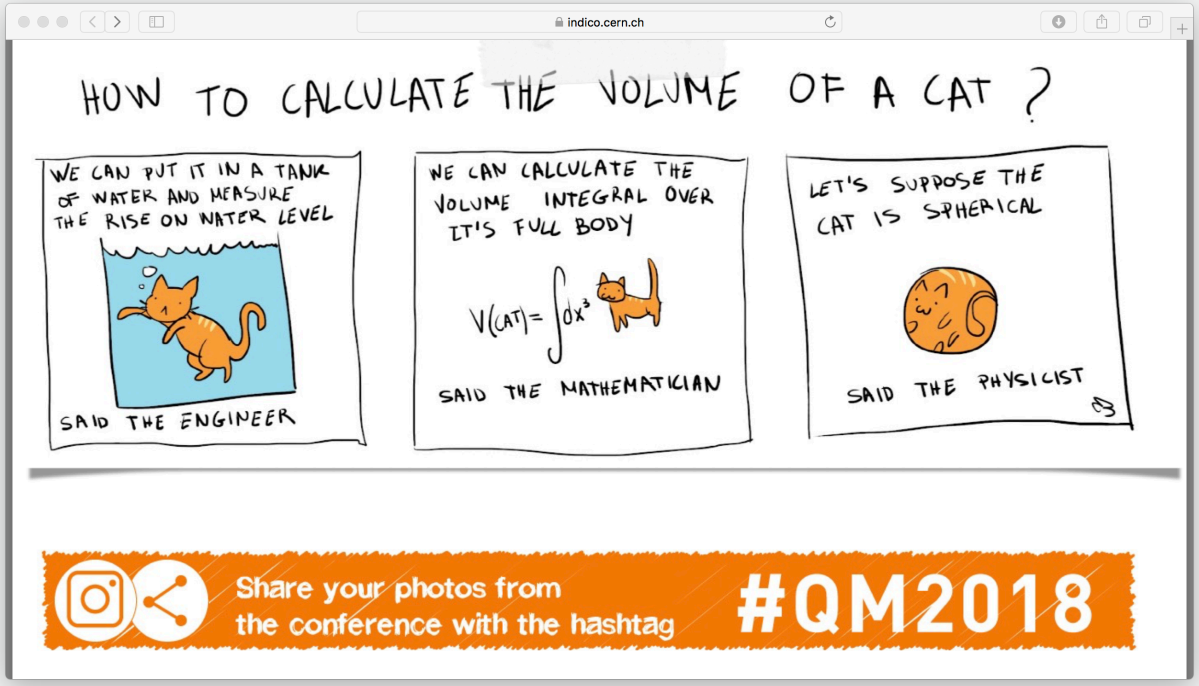

Instead of the WS densities, we use the densities obtained from the **density functional theory (DFT)** with parameter set SLy4.

Static model: Monte Carlo Glauber model

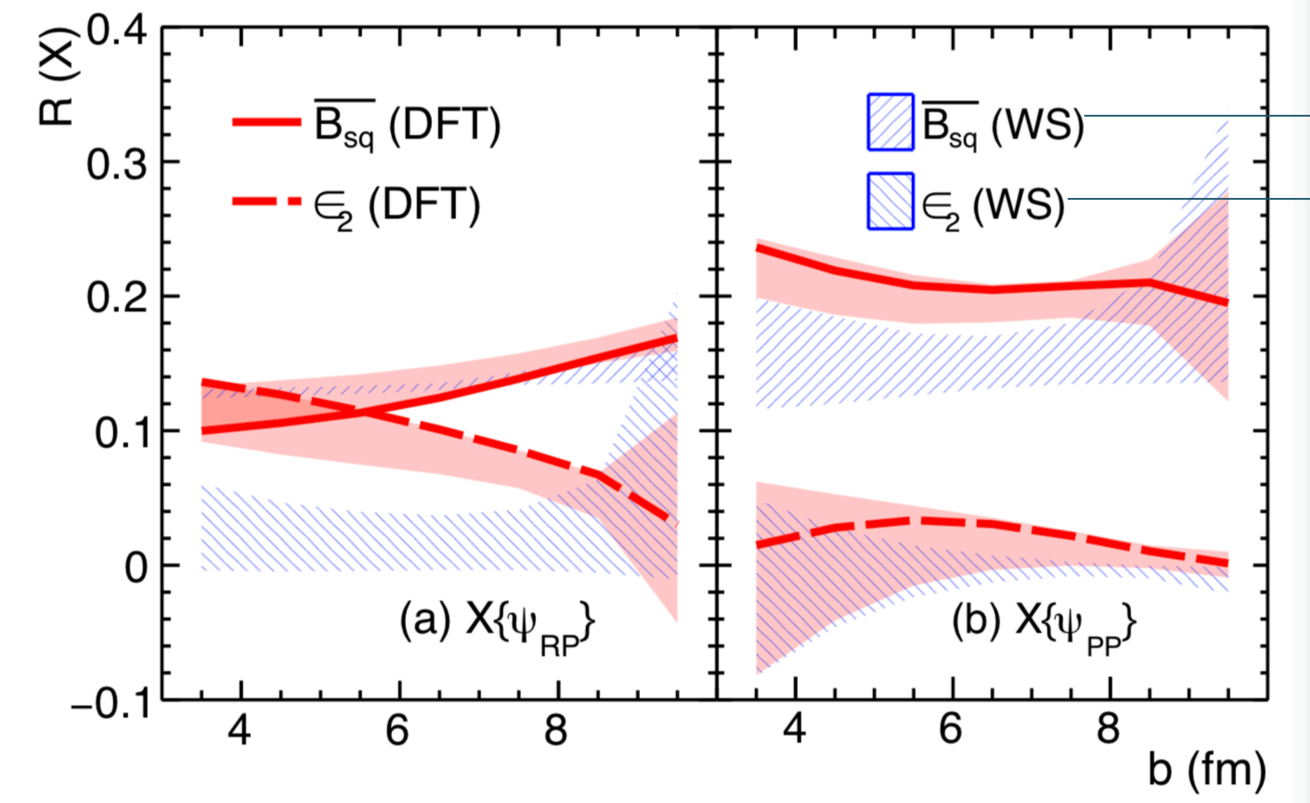

Signal

Background

Monte Carlo Glauber Model

$$R(X) \equiv 2(X_{\mathrm{RuRu}} - X_{\mathrm{ZrZr}})/(X_{\mathrm{RuRu}} + X_{\mathrm{ZrZr}}),$$

$$\epsilon_2\{\psi\} = \langle\langle \cos 2(\phi - \psi) \rangle\rangle$$

$$\overline{B_{sq}}\{\psi\} = \langle \int N_{part}^2(\mathbf{r})(eB(r,0)/m_\pi^2)^2 \cos 2(\psi_B - \psi) d\mathbf{r} / \int N_{part}^2(\mathbf{r}) d\mathbf{r} \rangle$$

AMPT simulations

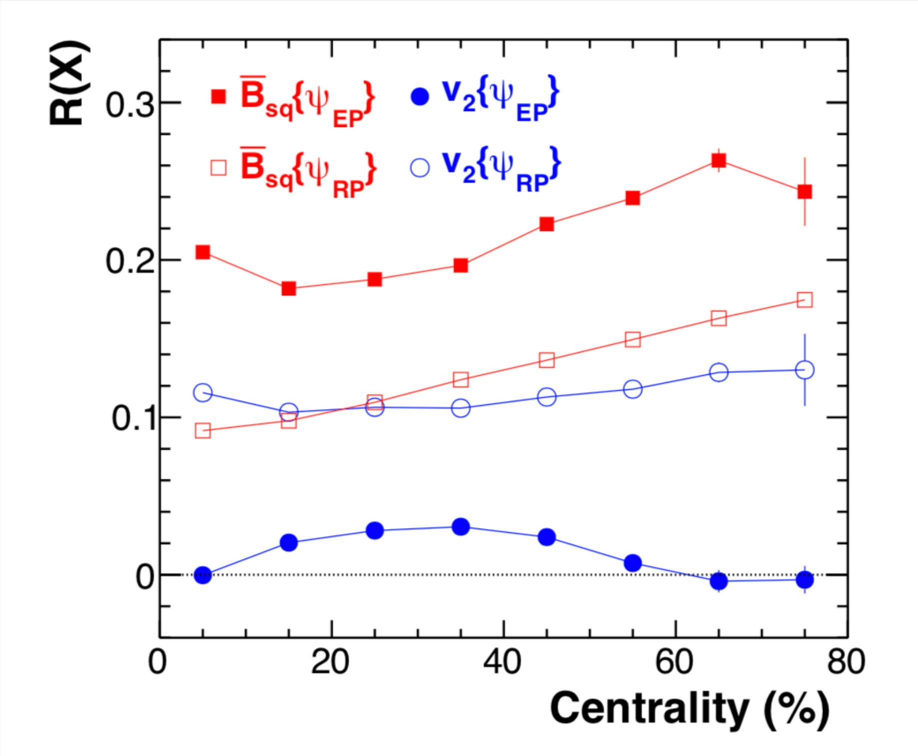

AMPT model

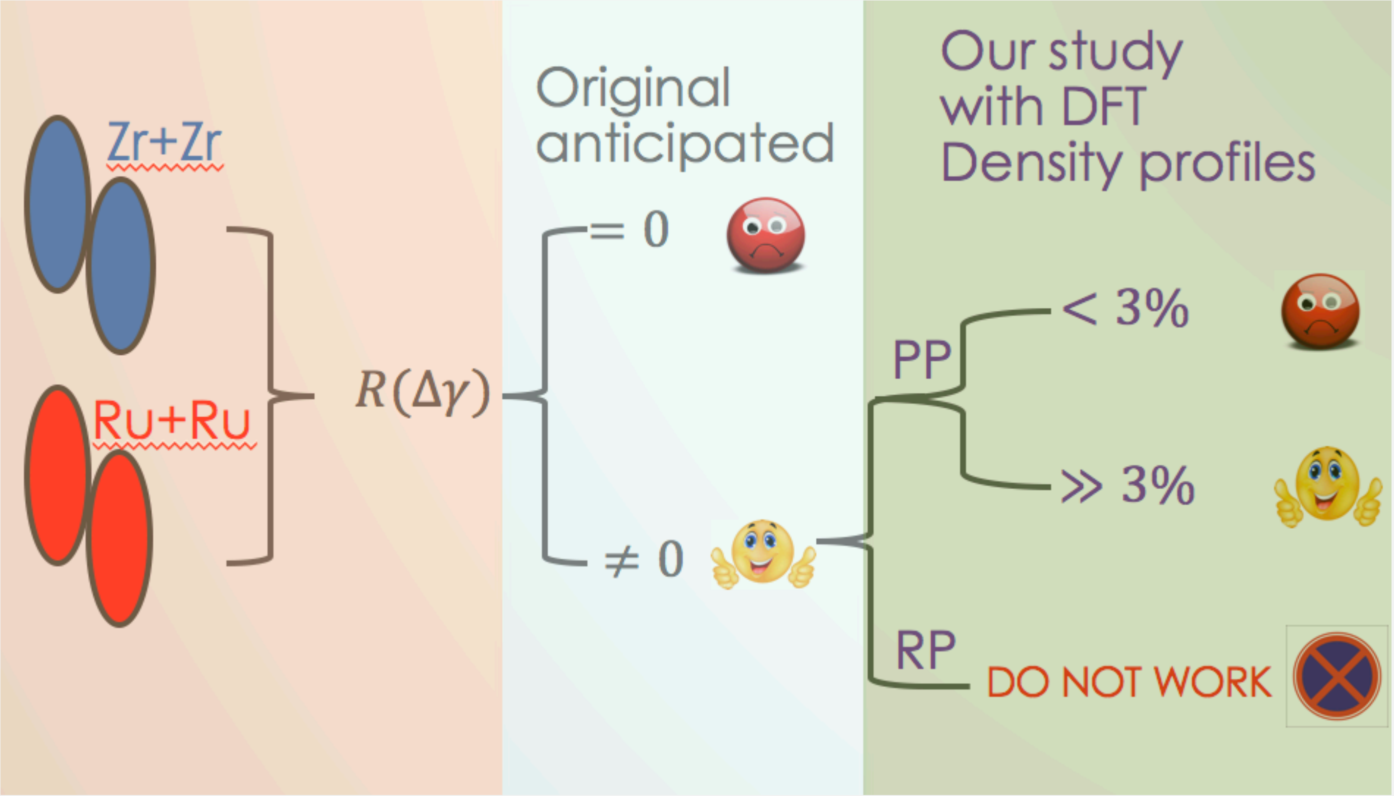

The expectations may **not hold as** originally anticipated because Zr+Zr collisions and Ru+Ru collisions may **have sizeable differences in v2**, thus the CME background

Multiplicity distributions

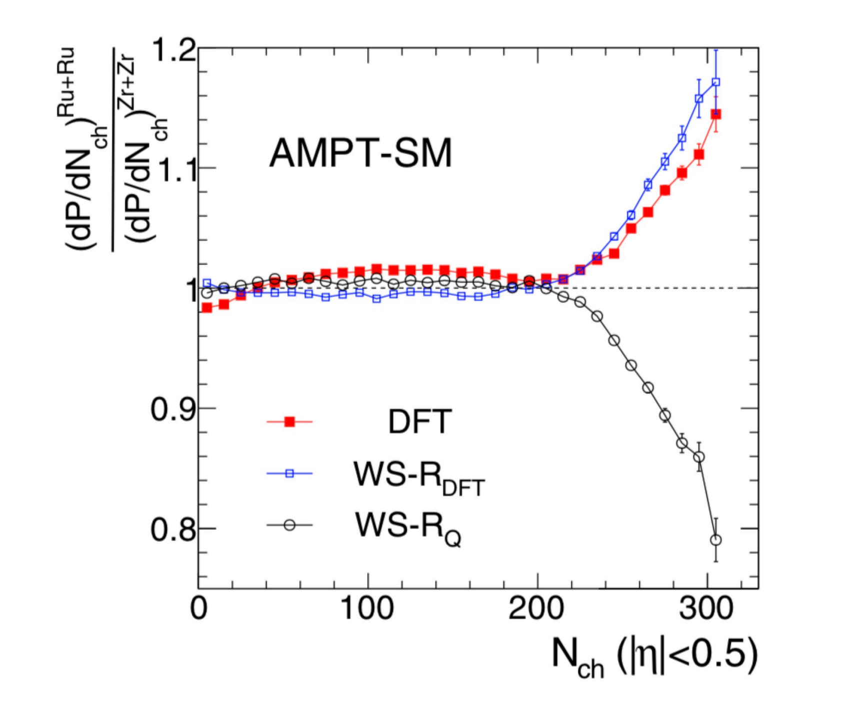

		$^{96}_{44}$Ru		$^{96}_{40}$Zr	
		Charge	mass	Charge	mass
WS-R_Q	R_0	5.085 [5]		5.020 [5]	
	$\sqrt{\langle r^2 \rangle}$	4.294		4.248	
DFT	$\sqrt{\langle r^2 \rangle}$	4.327	4.343	4.271	4.366
	$R_0 \equiv 1.183\sqrt{\langle r^2 \rangle}$	5.119	5.138	5.053	5.165

H. Li, et.al, PRC98, 054907 (2018)

- The **DFT** and **WS** densities give the **similar predictions** of the ratios of multiplicity distributions if the densities have same effective mass and charge radius.
- While the previous WS parameters extracted from charge density distributions give **opposite** behaviors of the ratio of multiplicity distributions .

neutron skin effect

III. Neutron skin and multiplicity distributions

H. Li, H. Xu, Y. Zhou, X. Wang, J. Zhao, L. Chen, F. Wang ,

“Probe the Neutron Skin with Ultrarelativistic Isobaric Collisions”

Physical Review Letters, in press
arXiv:1910.06170

Nuclear density distributions

SHF: Standard Skyrme-Hartree-Fock (SHF) model

eSHF: Extended SHF model

$$E(\rho,\delta) = E_0(\rho) + E_{sym}(\rho)\delta^2 + O(\delta^4)$$

$$\rho = \rho_n + \rho_p;\ \ \delta = \frac{\rho_n - \rho_p}{\rho};\ \ \rho_c \simeq 0.11 fm^{-3}$$

$$L(\rho_c) = 3\rho_c \left[\frac{dE_{sym}(\rho)}{d\rho}\right]_{\rho=\rho_c}$$

Z. Zhang, PRC94, 064326(2016)

$$\begin{aligned} v_{i,j} &= t_0(1+x_0P_\sigma)\delta(\boldsymbol{r}) + \frac{1}{6}t_3(1+x_3P_\sigma)\rho^\alpha(\boldsymbol{R})\delta(\boldsymbol{r}) \\ &+ \frac{1}{2}t_1(1+x_1P_\sigma)[K'^2\delta(\boldsymbol{r}) + \delta(\boldsymbol{r})K^2] \\ &+ t_2(1+x_2P_\sigma)\boldsymbol{K}'\cdot\delta(\boldsymbol{r})\boldsymbol{K} \\ &+ \frac{1}{2}t_4(1+x_4P_\sigma)[K'^2\delta(\boldsymbol{r})\rho(\boldsymbol{R}) + \rho(\boldsymbol{R})\delta(\boldsymbol{r})K^2] \\ &+ t_5(1+x_5P_\sigma)\boldsymbol{K}'\cdot\rho(\boldsymbol{R})\delta(\boldsymbol{r})\boldsymbol{K} \\ &+ iW_0(\boldsymbol{\sigma}_i+\boldsymbol{\sigma}_j)\cdot[\boldsymbol{K}'\times\delta(\boldsymbol{r})\boldsymbol{K}], \qquad (4) \end{aligned}$$

Extended

	eSHF			SHF
	Lc20	Lc47	Lc70	SLy4
$L(\rho_c)$(MeV)	20.000	47.300	70.000	42.661
$E_{\rm sym}(\rho_c)$(MeV)	26.650	26.650	26.650	26.450
ρ_0(fm^{-3})	0.15414	0.15267	0.15059	0.15954
t_0(MeV · fm^3)	−2063.0	−2037.3	−1855.3	−2488.9
t_1(MeV · fm^5)	442.48	524.18	576.91	486.82
t_2(MeV · fm^5)	−562.02	−521.60	−76.702	−54.640
t_3(MeV · fm$^{3+3\alpha}$)	14726.	13734.	12367.	13777.
t_4(MeV · fm$^{5+3\beta}$)	−1532.5	−1615.7	−1650.2	-
t_5(MeV · fm$^{5+3\gamma}$)	3037.5	2153.2	−436.51	-
x_0	0.92728	0.29070	−0.26752	0.83400
x_1	1.3163	0.37275	−0.51268	−0.34400
x_2	−0.55463	−0.55121	3.1558	−1.00000
x_3	0.98695	0.13143	−0.83906	1.35400
x_4	1.7600	0.29499	−1.5709	-
x_5	−0.83852	−0.65206	−4.1683	-
α	0.28356	0.27858	0.31853	0.16667
β	1	1	1	-
γ	1	1	1	-
W_0(MeV · fm^5)	92.759	100.14	113.61	123.00

Additional density-dependent two-body forces to effectively simulate the momentum-dependent three-body forces

Neutron skin thickness

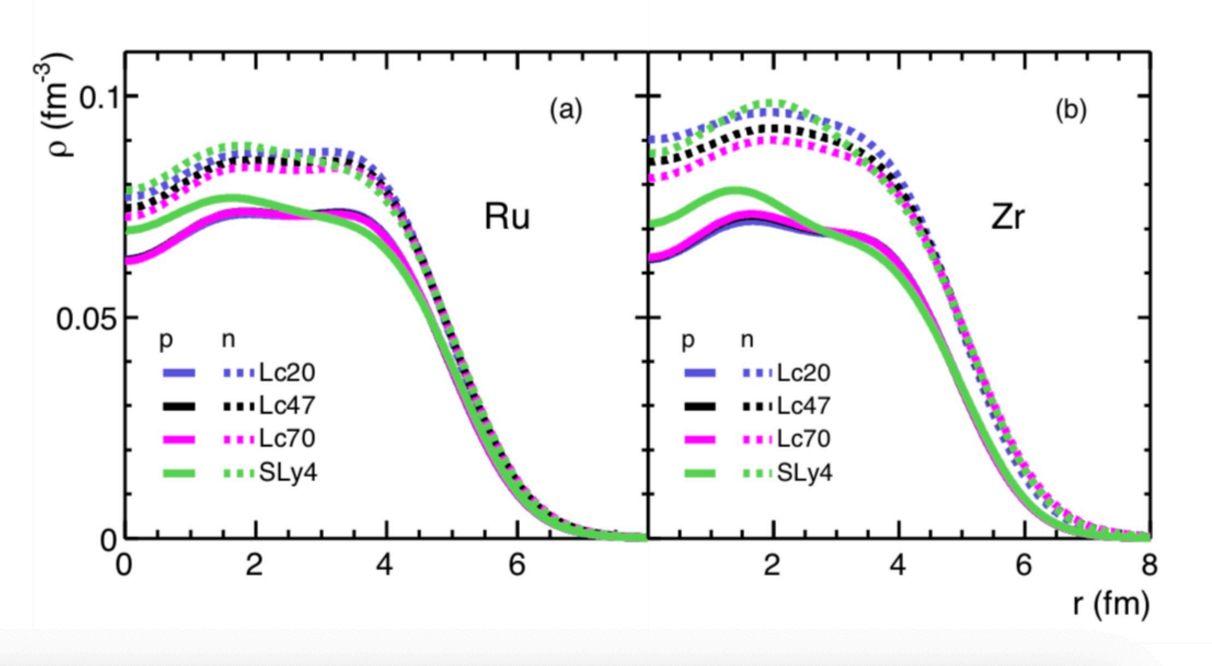

	$L(\rho_c)$	$L(\rho_0)$	^{96}Zr r_n	r_p	Δr_{np}	^{96}Ru r_n	r_p	Δr_{np}	^{208}Pb Δr_{np}
Lc20	20	13.1	4.386	4.27	0.115	4.327	4.316	0.011	0.109
Lc47	47.3	55.7	4.449	4.267	0.183	4.360	4.319	0.042	0.190
Lc70	70	90.0	4.494	4.262	0.232	4.385	4.32	0.066	0.264
SLy4	42.7	46.0	4.432	4.271	0.161	4.356	4.327	0.030	0.160

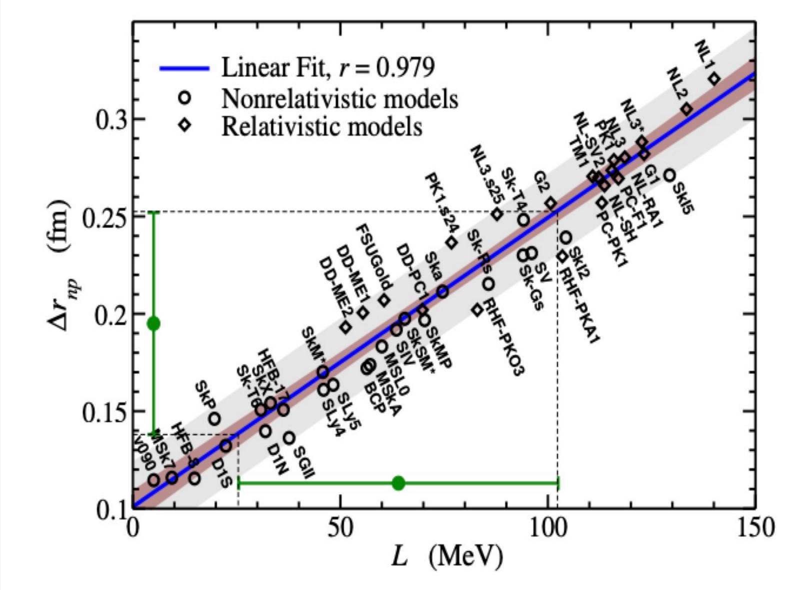

$$\sqrt{\langle r^2\rangle} = \sqrt{\int \rho(r) r^4 dr / \int \rho(r) r^2 dr} \qquad \Delta r_{np} = r_n - r_p$$

The four interactions give similar proton rms, but the neutron radius increase with $L(\rho_c)$

Roca-Maza, PRL106, 252501 (2011)

Heavy ion event generators

- Heavy ion jet interaction generator (Hijing)
- A Multi-Phase Transport model (AMPT)
  - Default (String fragmentation)
  - String melting
- Ultra relativistic Quantum Molecular Dynamics (UrQMD)

Multiplicity distributions

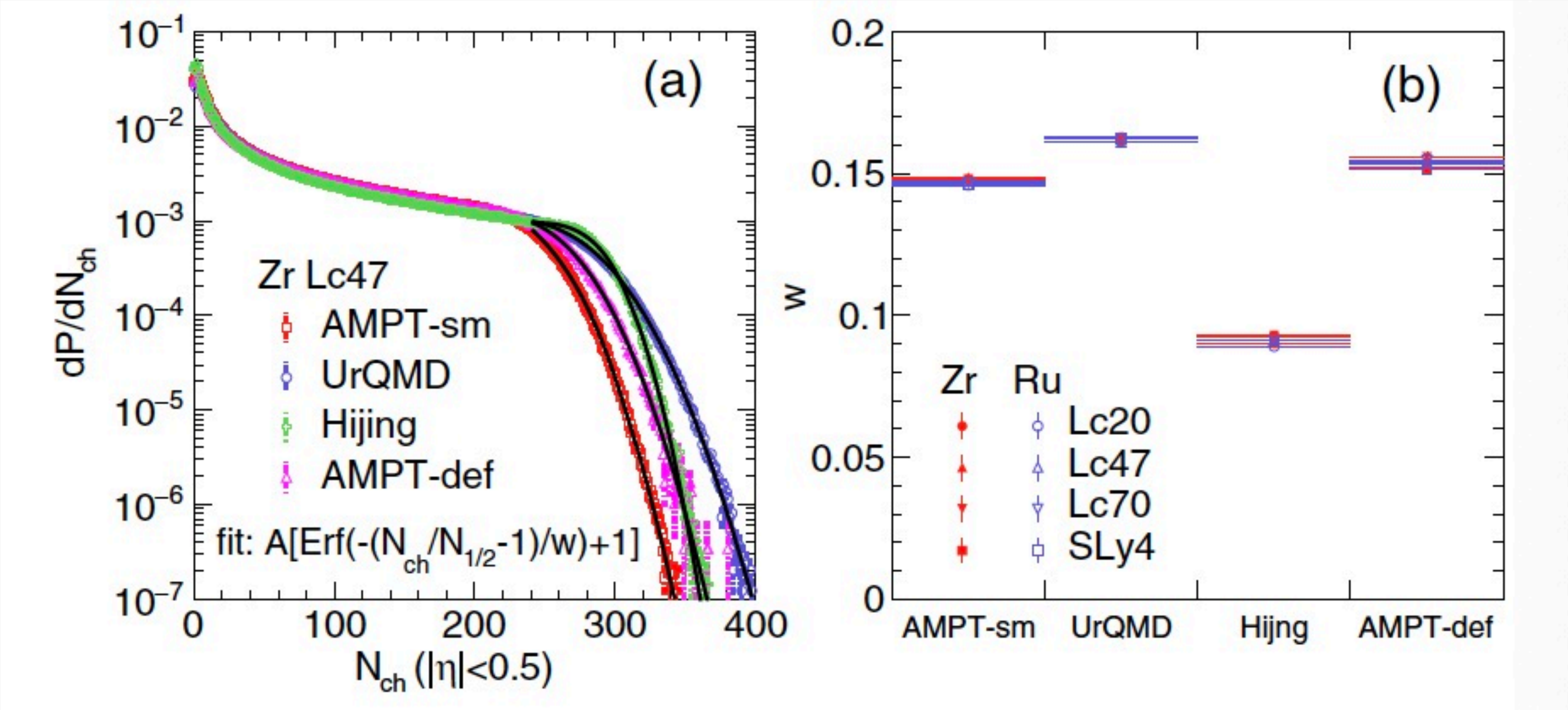

$$dP/dN_{\mathrm{ch}} \propto -\mathrm{Erf}[-(N_{\mathrm{ch}}/N_{1/2} - 1)/w] + 1, \qquad (1)$$

The effect is hardly observable in a plot of the N_{ch} distributions themselves.

Ratios of N_{ch} distributions

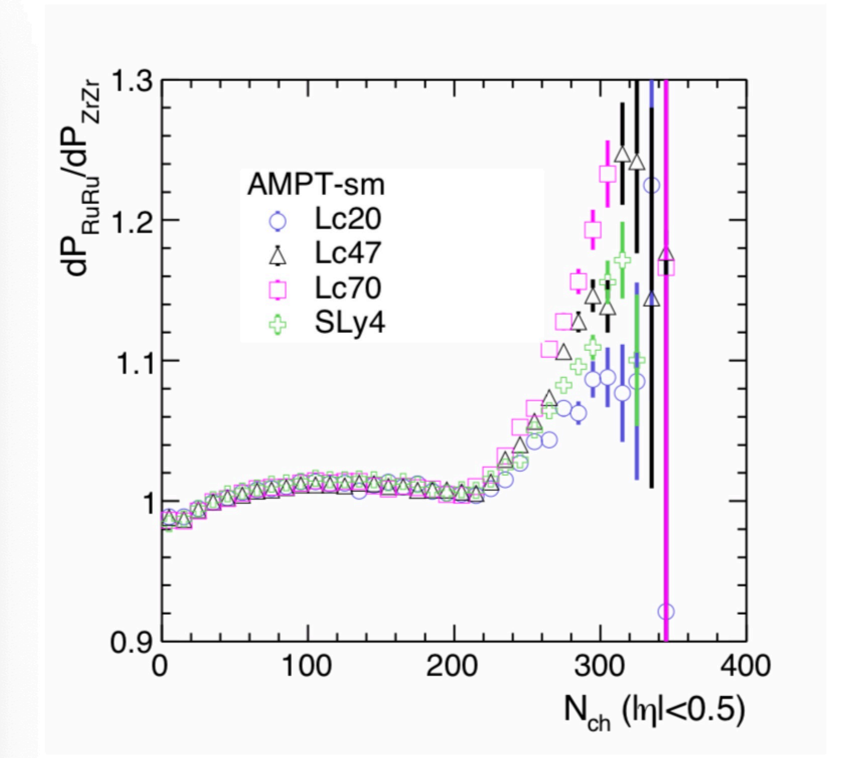

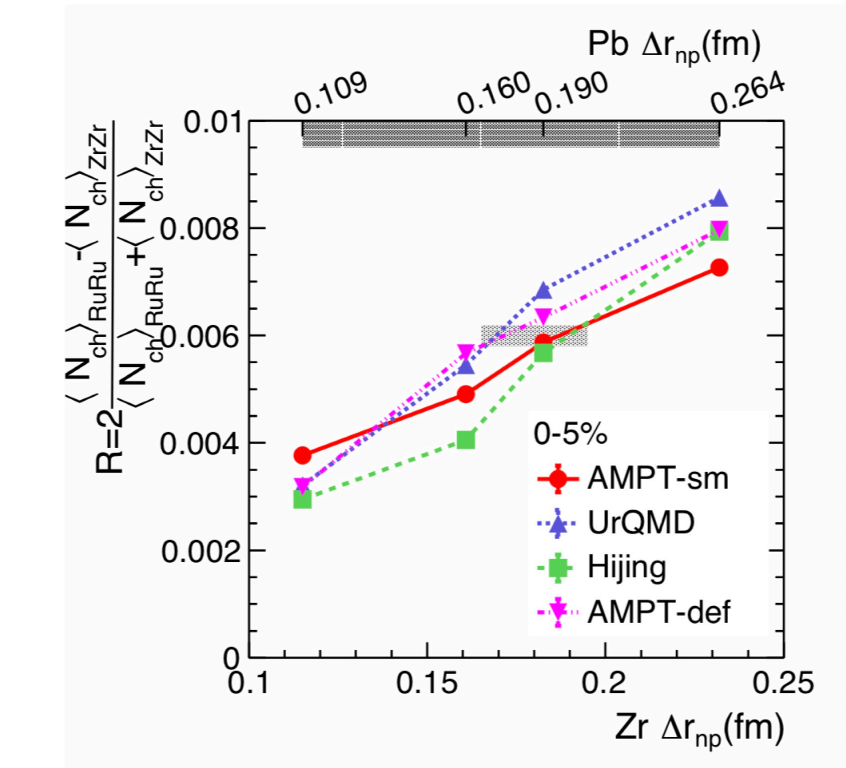

- The ratio of N_{ch} distributions highlight the differences but cumbersome to quantify
- To quantify the differences, we use the R observable of $\langle N_{ch}\rangle$ at top 5% centrality.

Neutron skin and particle production

Pb+Pb 400 Mev/nucleon

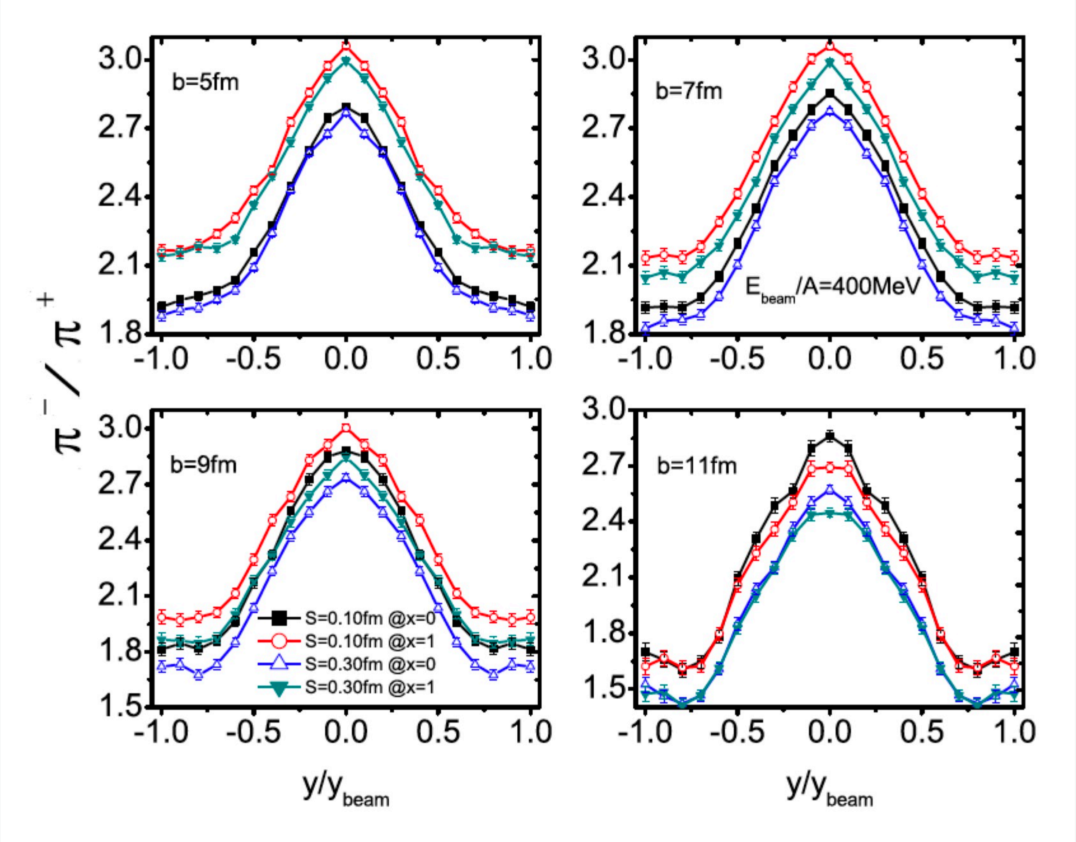

Pb+Pb 1000 Mev/nucleon

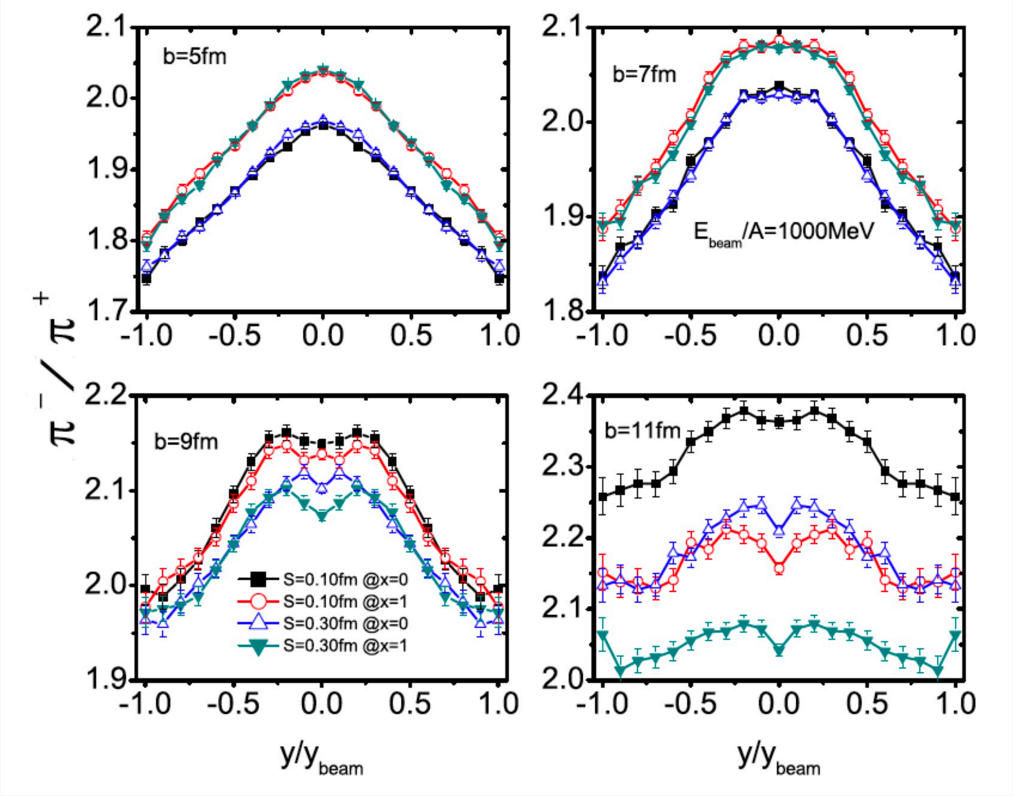

G. Wei, et.al, PRC90, 014610 (2014)

Isospin-sensitive observable

The R observable

R is a relative measure, **much of experimental effects cancel:**

1. **Track inefficiency**: We use only 0-5% central collisions , where the tracking efficiency is constant to a good degree
2. **Trigger inefficiency**: the trigger inefficiency can be corrected in experiment. Even without correction, the uncertainty is about 2×10^{-4}, negligible small.

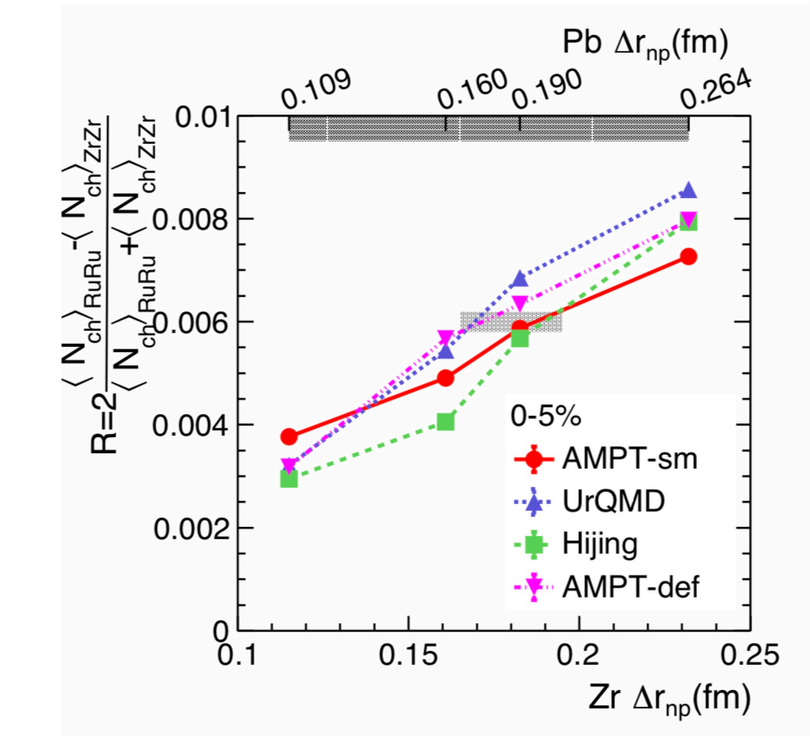

Question: The R observable is actually a isospin insensitive observable, why it have **rather weak model dependence**?

The particle production in relativistic heavy ion collisions **is insensitive to the details of the QCD physics**, which is in contrast to the hadronic observables in low-energy studies.

Static models

- **Glauber model**

$$\frac{dN}{dy} \propto s \propto \frac{(1-x)}{2} n_{part} + x n_{coll}$$

n_{part}: number of participant; n_{coll}: number of binary collisions

$$x = 0.1(\text{default}),\ x = 0.2(\text{extreme})$$

- **Trento model** (J. Moreland, et.al, PRC92, 011901(2015))

$$\frac{dN}{dy} \propto s \propto \left(\frac{T_A^p + T_B^p}{2}\right)^{1/p}\ ;\ p = 0 \text{ and } k = 1.4$$

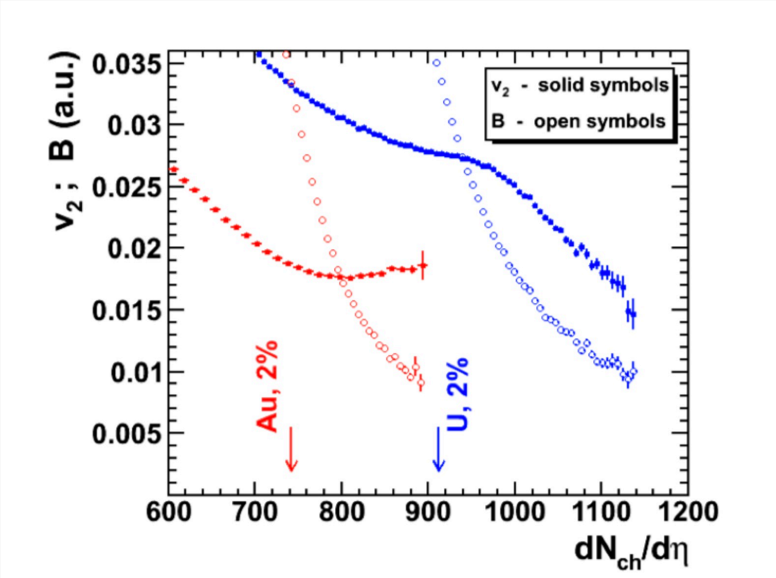

Voloshin, PRL105, 172301 (2010)

No knee structure in data

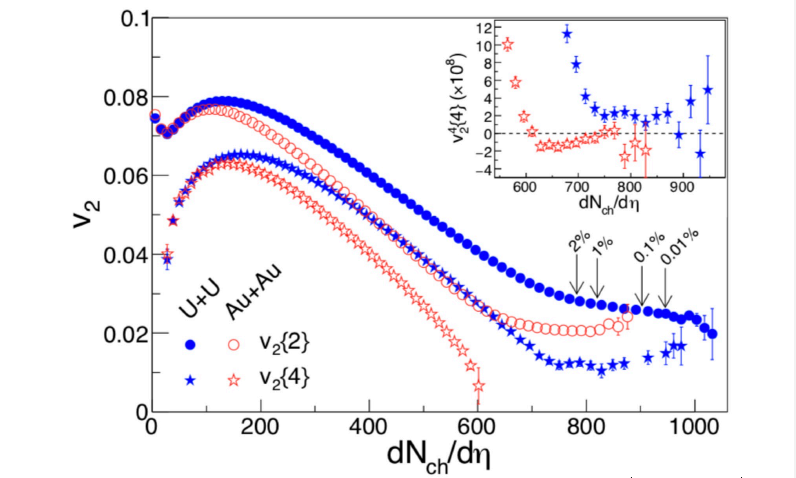

STAR, PRL115, 222301 (2015)

Probe the neutron skin thickness

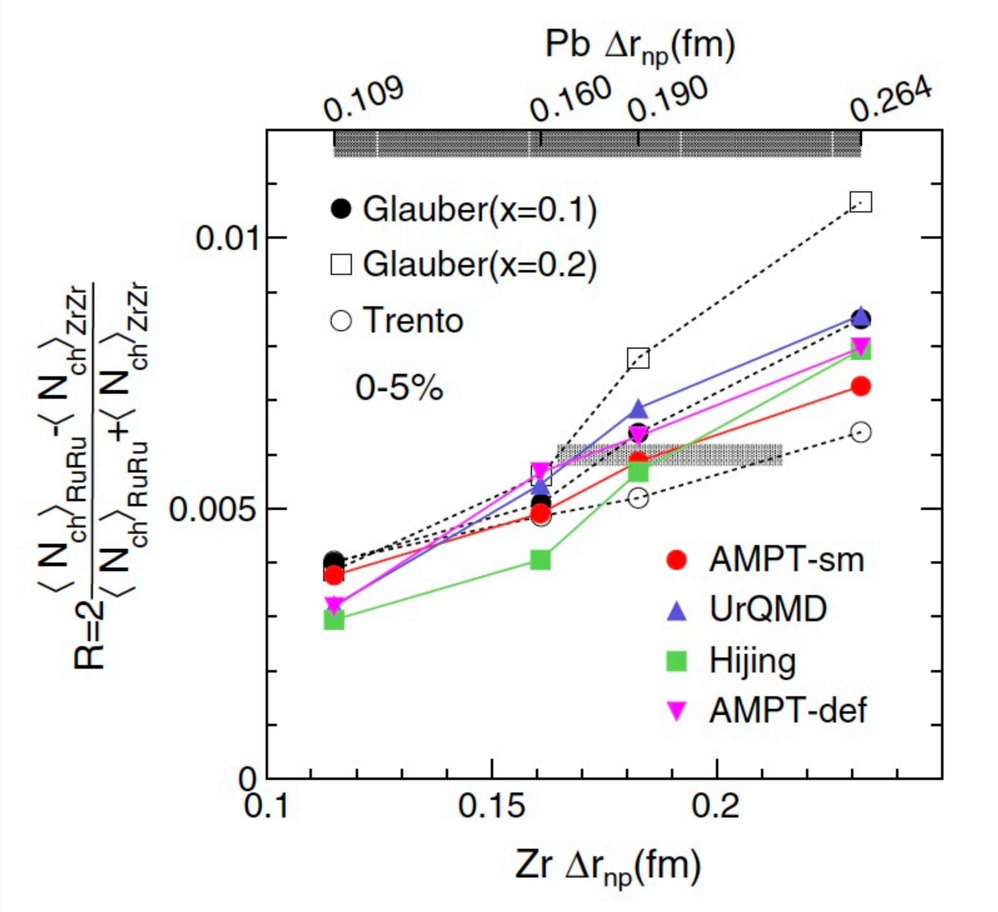

4 dynamic models + 2 static models

The R observable in isobaric collisions at ultra-relativistic energies provide a novel approach to determine the neutron skin thickness to a precision that may comparable to or even exceed those achieved by traditional low-energy nuclear experiments.

STAR isobar collisions (2018):

- More statistics: 6.3 billion isobar events
- Less systematical uncertainty

Summary

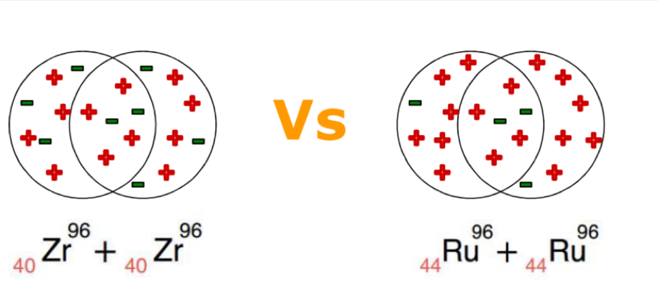

v_2

CME☹

H. Xu, et.al, PRL121, 022301 (2018)
arXiv: 1710.03086

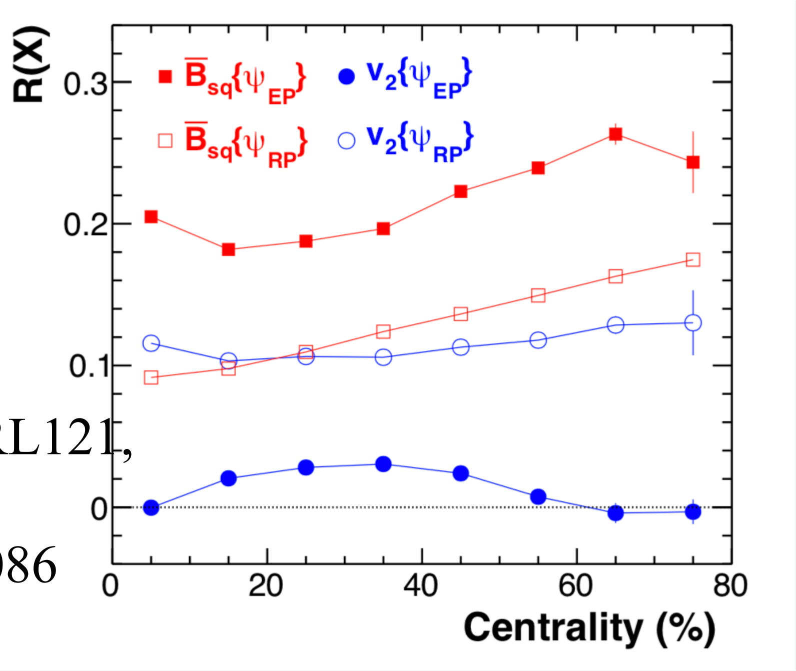

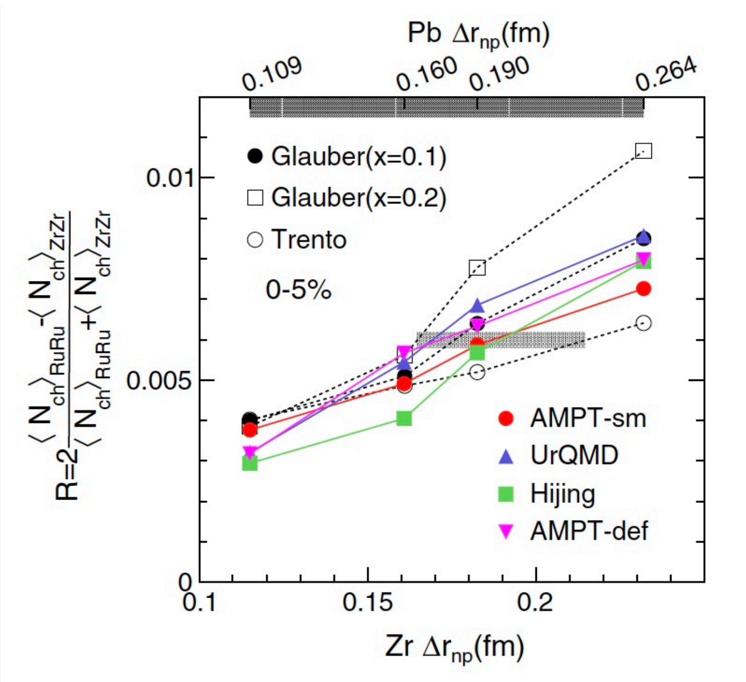

H. Li, et.al, PRL in press (2020)
arXiv:1910.06170

$\langle N_{ch}\rangle$

Neutron skin🙂

- The effect of nuclear densities on the relative differences of v_2 and $\langle N_{ch}\rangle$ in isobaric collisions are investigated.
- Such a premise may already be in stock in the isobar collision data taken at RHIC in 2018.

Thank you for your attention!

"When one door closes, another door opens, but we so often look so long and so regretfully upon the closed door, that we do not see the ones which open for us."

– Alexander Graham Bell